Phys.Lett.B 687:11-15,2010

Photoproduction of meson pairs: First measurement of the polarization observable I^s

Abstract

The polarization observable I^s, a feature exclusive to the acoplanar kinematics of multi-meson final states produced via linearly polarized photons, has been measured for the first time. Results for the reaction $\vec{\gamma}p \to p\pi^0\eta$ are presented for incoming photon energies between 970 MeV and 1650 MeV along with the beam asymmetry I^c. The comparably large asymmetries demonstrate a high sensitivity of I^s to the dynamics of the reaction. The sensitivity of these new polarization observables to the contributing partial waves is demonstrated by fits using the Bonn-Gatchina partial wave analysis.

PACS: 13.60.-r, 13.60.Le, 13.88.+e

На конкурс ПИЯФ 2010 года.
Работа представляется В.В.Сумачёвым.

Эксперименты на электронном ускорителе ELSA.

The CBELSA/TAPS Collaboration

E. Gutz[a,1], V. Sokhoyan[a], H. van Pee[a], A.V. Anisovich[a,b], J.C.S. Bacelar[c], B. Bantes[d], O. Bartholomy[a], D. Bayadilov[a,b], R. Beck[a], Yu. Beloglazov[b], R. Castelijns[c], V. Crede[a,g], H. Dutz[d], D. Elsner[d], R. Ewald[d], F. Frommberger[d], M. Fuchs[a], Ch. Funke[a], R. Gregor[e], A. Gridnev[b], W. Hillert[d], Ph. Hoffmeister[a], I. Horn[a], I. Jägle[f], J. Junkersfeld[a], H. Kalinowsky[a], S. Kammer[d], V. Kleber[d,2], Frank Klein[d], Friedrich Klein[d], E. Klempt[a], M. Kotulla[e,f], B. Krusche[f], M. Lang[a], H. Löhner[c], I. Lopatin[b], S. Lugert[e], D. Menze[d], T. Mertens[f], J.G. Messchendorp[c], V. Metag[e], M. Nanova[e], V. Nikonov[a,b], D. Novinski[b], R. Novotny[e], M. Ostrick[d,3], L. Pant[e,4], M. Pfeiffer[e], D. Piontek[a], W. Roberts[g], A. Roy[e,5], A. Sarantsev[a,b], S. Schadmand[e,6], Ch. Schmidt[a], H. Schmieden[d], B. Schoch[d], S. Shende[c], A. Süle[d], V. Sumachev[b], T. Szczepanek[a], A. Thiel[a], U. Thoma[a,1], D. Trnka[e], R. Varma[e,5], D. Walther[d], Ch. Weinheimer[a,7], Ch. Wendel[a]

Эксперименты на электронном ускорителе ELSA.

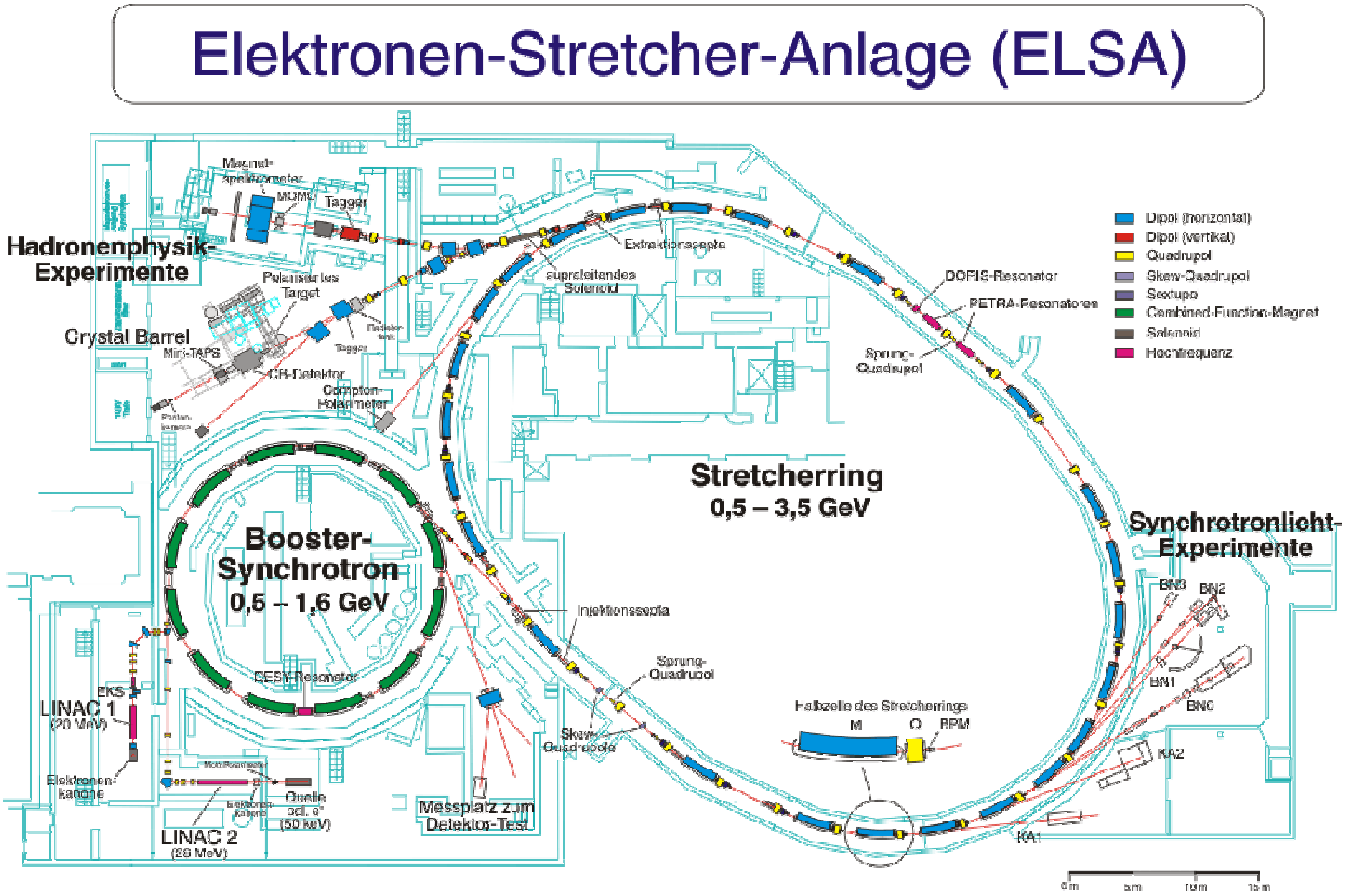

Эксперименты на электронном ускорителе ELSA.

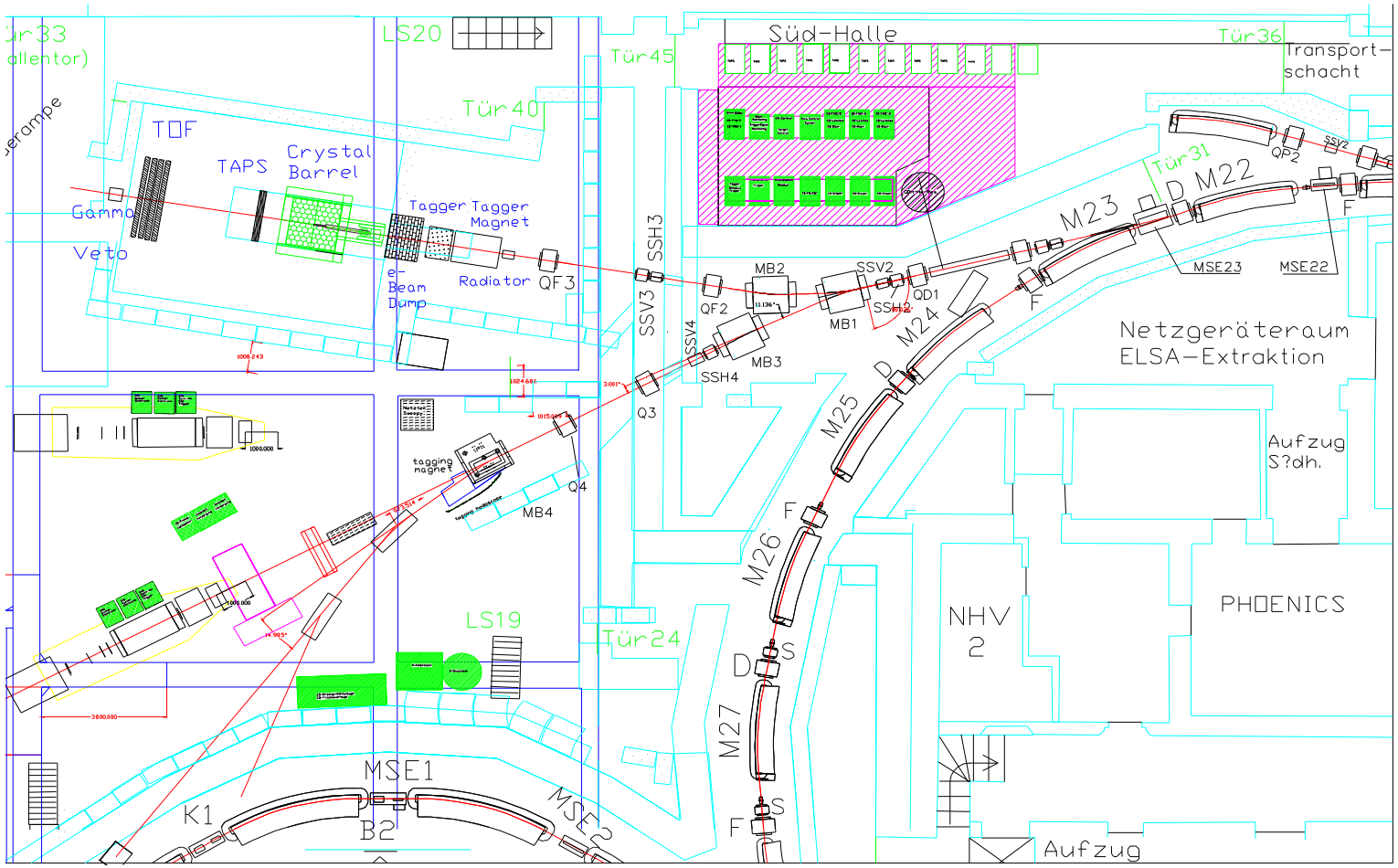

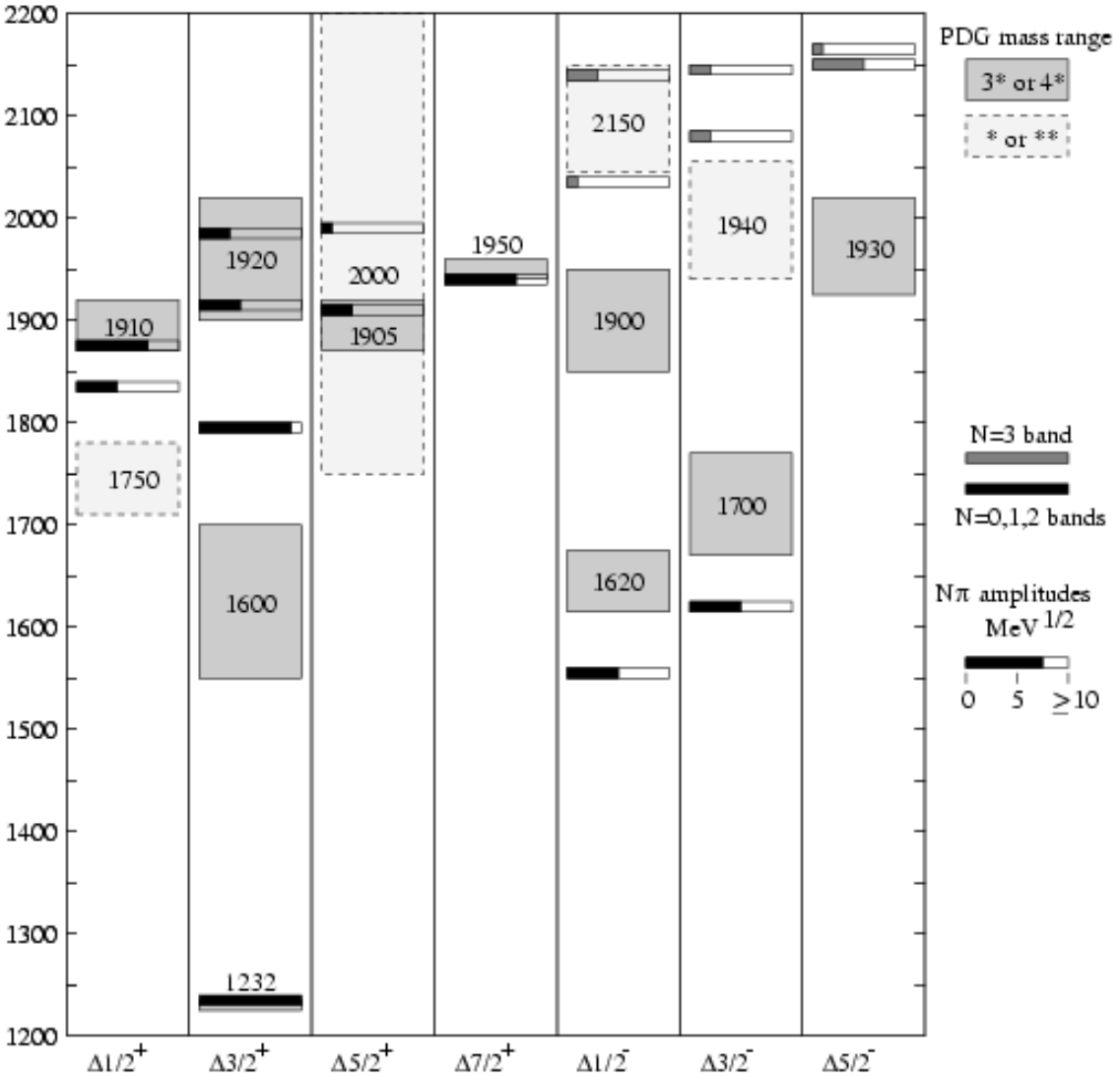

FIG. 10. Model masses and $N\pi$ decay amplitudes for Δ resonances below 2200 MeV from Refs. [56,61], compared to the range of central values for resonances masses from the PDG [3]. Caption as in Fig. 9.

S.Capstick, W Roberts, Prog.Part.Nucl.Phys. 45, 241 (2000).

The Δ^*- states

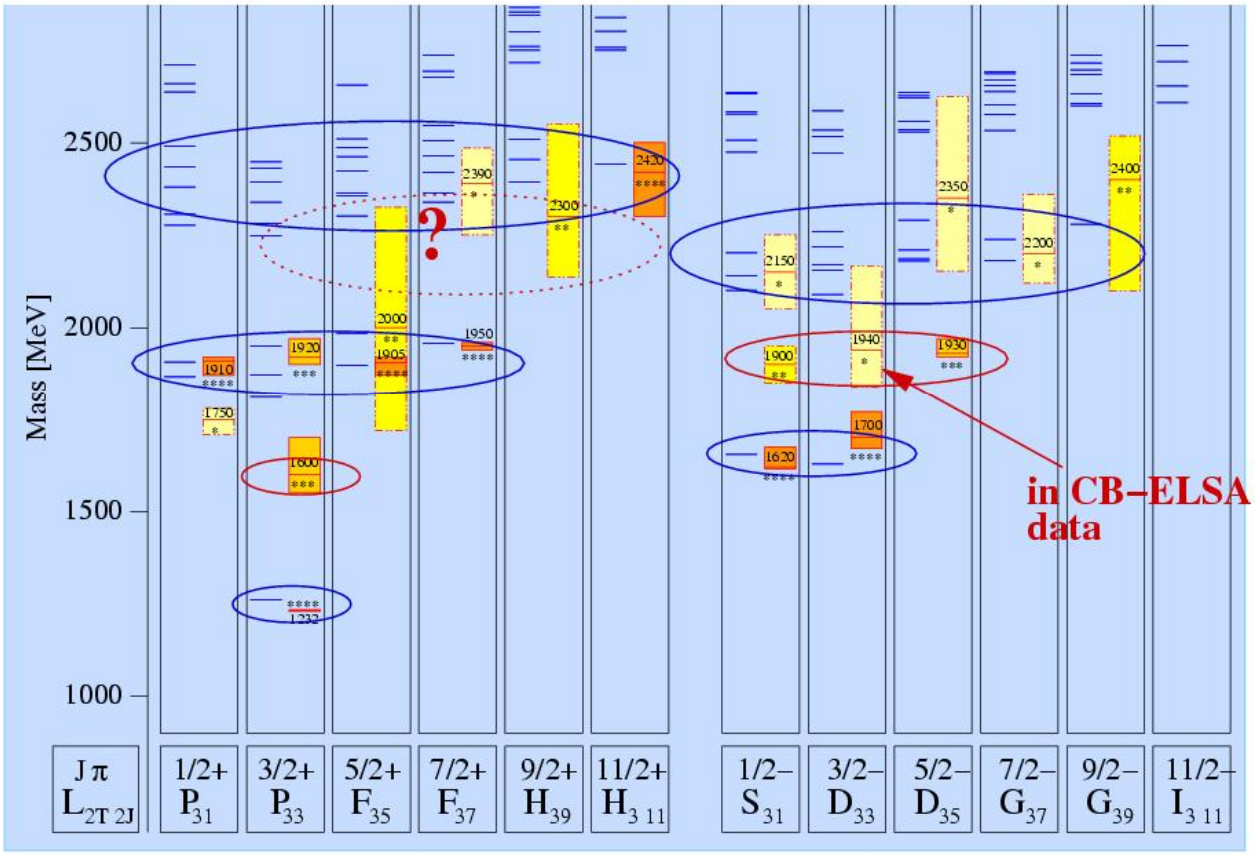

Quark model
U. Löring, B. Metsch, H. Petry et al.

model
$\sim 2n + \ell$

data
$\sim n + \ell$?

$\leftrightarrow$ Parity doublets ?

$\Leftrightarrow$ Additional experimental information needed !!

Схема установки.

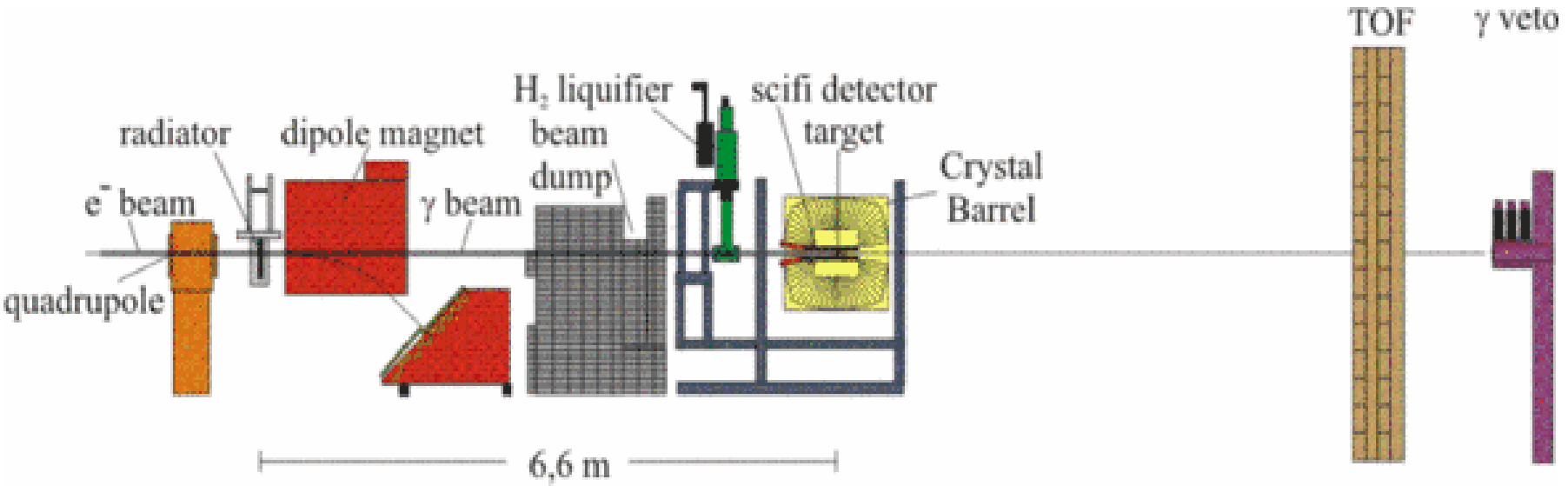

Экспериментальный зал.

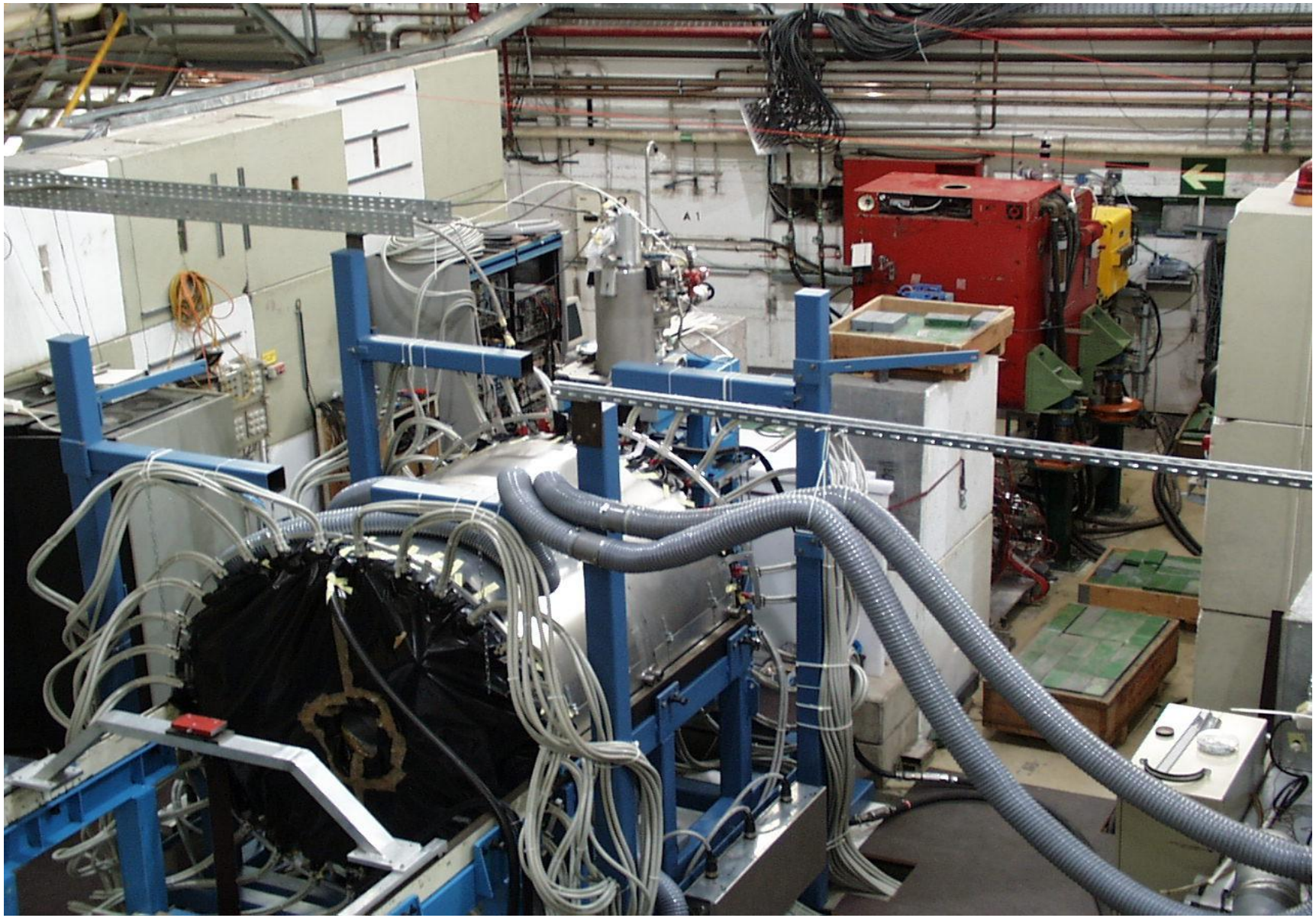

Main Contribution to the Project

- **Radiator and Goniometer (Bonn)**
- **Tagger with PWC and Fibre detector (Bonn, Gatchina)**
- **Inner Fibre Detector (Erlangen)**
- **Crystal Barrel (Bonn)**
- **Taps (Basel, Giessen, Groningen)**
- **TOF (Bonn)**
- **EMS (Bonn)**
- **Hydrogen Target (Bonn,Dresden)**
- **Cluster Trigger Processor (Bochum)**
- **Data Acquisition (Bonn)**

3 amorphous Radiator Targets

Cu 1/100 [X_0] d = 150 μm
Cu 3/100 [X_0] d = 450 μm
Cu 3/1000 [X_0] d = 40 μm
Empty Position
Beam Diagnosis Screen

1 Crystal Radiator Target

Diamond Crystal 4/1000 [X_0] d = 500 μm

View of Radiator Target

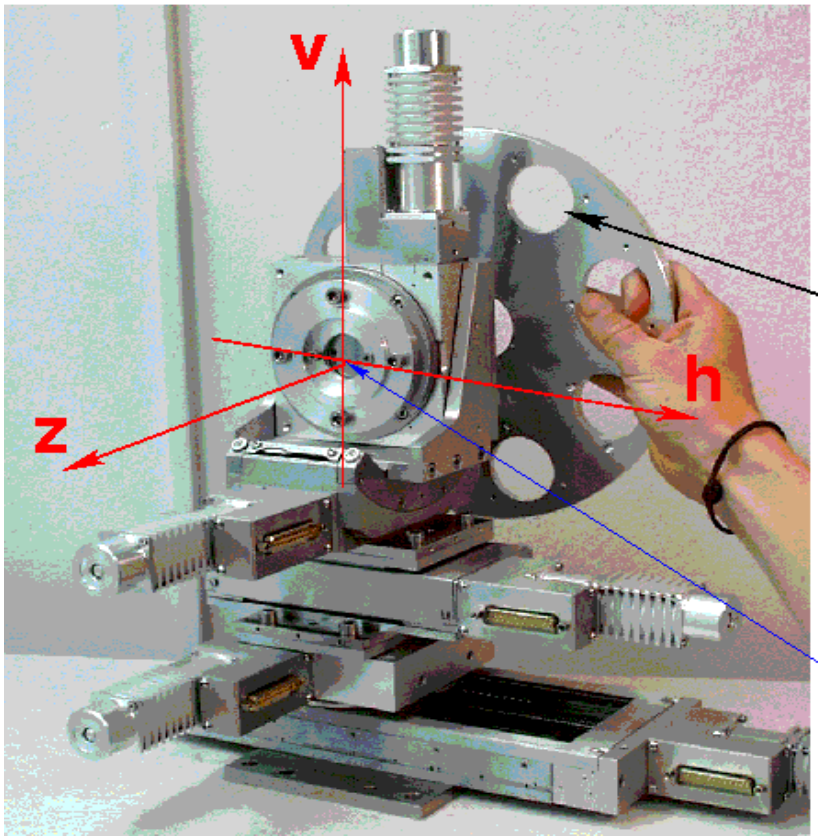

amorphous radiators

screen

empty position

wires for determination of beam profiles

diamont crystal

Tagger System

14 Scintillator (fast Trigger)

2 PWC (Position determination,

4 mm Wire Spacing,

350 Wires)

480 Scintillating Fibres (High Rates, Multi Hit TDC,

2mm Fibre Diameter)

Range: 95% to 25% of Electron Beam Momentum

Resolution: 0,03% to 2.8%

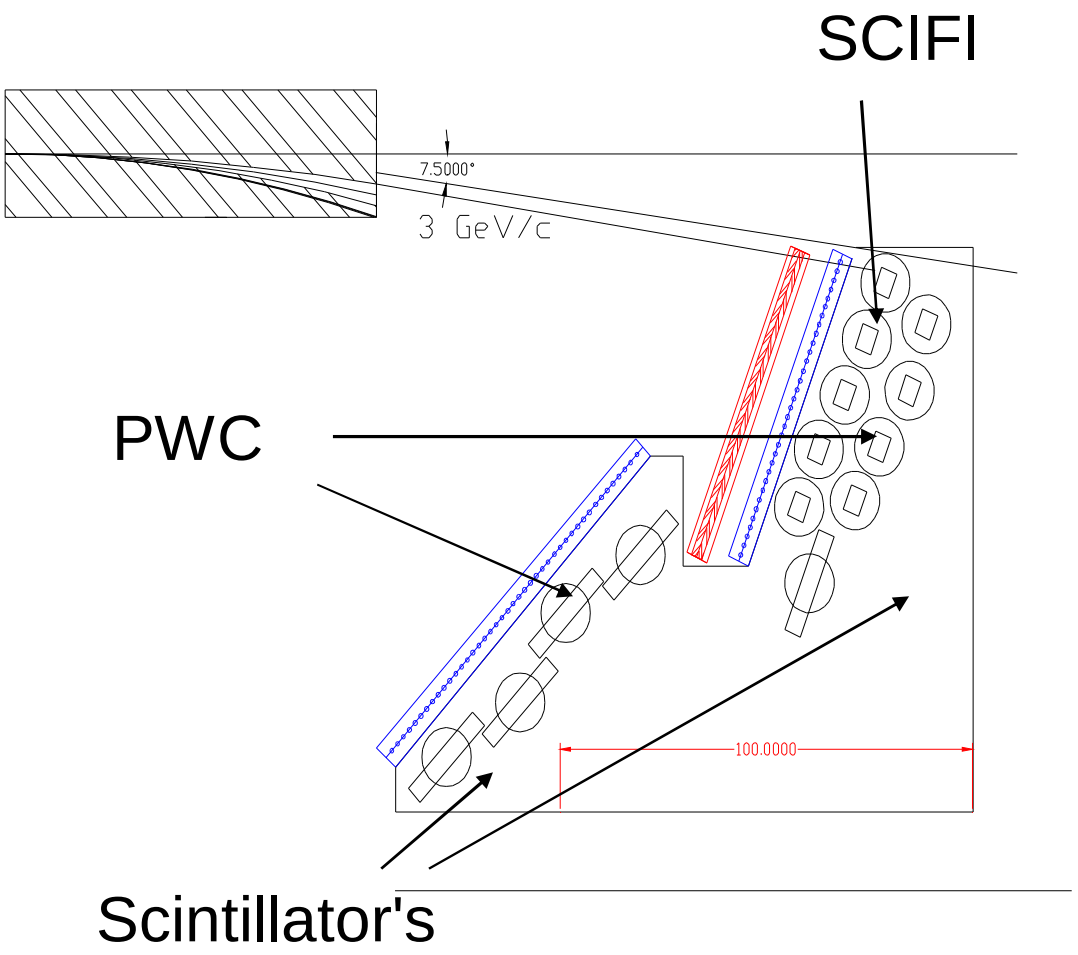

Photon Production via Bremsstrahlung

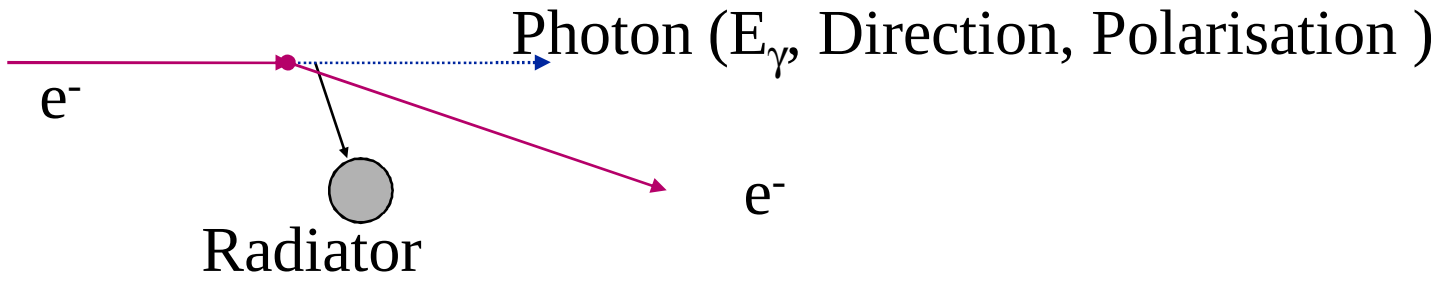

$$W_\gamma\left(E_\gamma, E_e\right) := \frac{1}{X_0}\cdot\frac{1}{E_\gamma}\cdot F\left(E_e, E_\gamma\right)\cdot dx\ dE_\gamma$$

$$F\left(E_e, E_\gamma\right) := 1$$

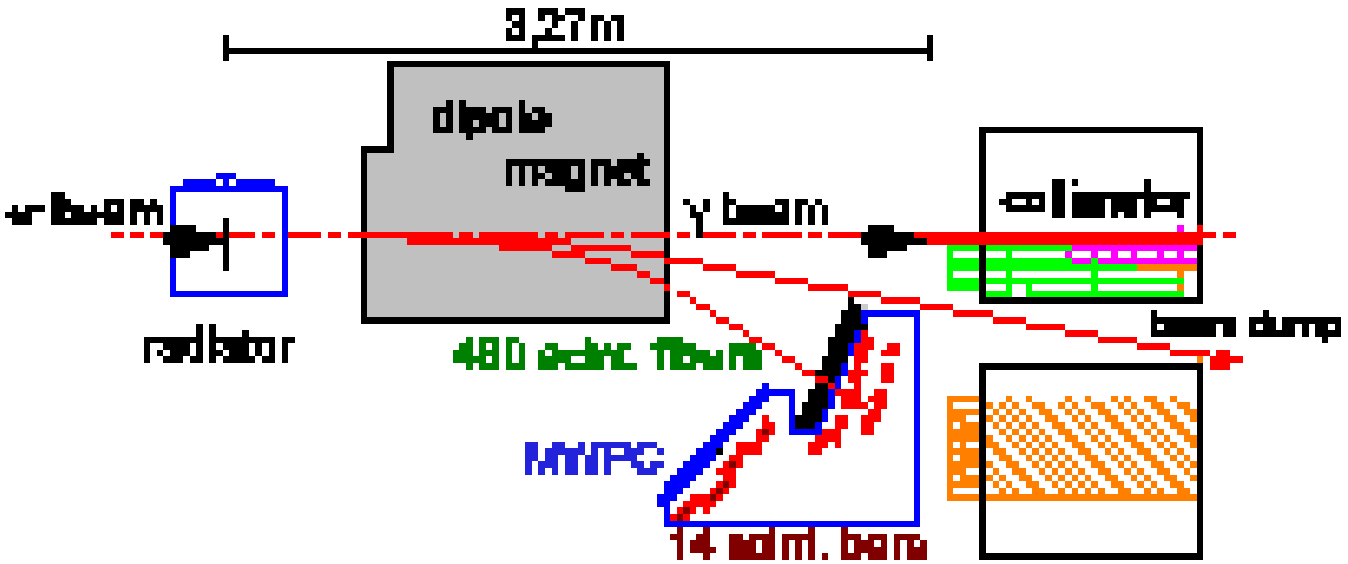

Fig. 8. Setup of the tagging system as described in the text.

electron energy	5176.1 MeV
rms beam size $\sigma_{x,\mathrm{rms,natural}}$	1.3 mm
rms beam size $\sigma_{y,\mathrm{rms,natural}}$	1.0 mm
divergence rms $\sigma'_{x,\mathrm{rms,natural}}$	0.3 mrad
divergence rms $\sigma'_{y,\mathrm{rms,natural}}$	0.04 mrad

Table 1. Electron beam properties.

crystal thickness	0.5 mm
calculated number of lattice vectors	1000
bandwidth scaling factor	1.35

Table 2. Radiator properties.

$E_\gamma(I^{pol,max})$/MeV	$I^{pol,max}$	θ_x^{CV}/mrad	θ_y^{CV}/mrad
1305	0.49	-3.16	-36.78
1515	0.42	-4.09	-44.00
1610	0.39	-4.58	47.00
1814	0.31	-5.88	76.00

Table 3. Coherent peak position, maximum degree of polarization, $I^{pol,max}$, and crystal angles for the vertical orientation of the polarization plane.

Fast Forward Photon Detector with PM Readout

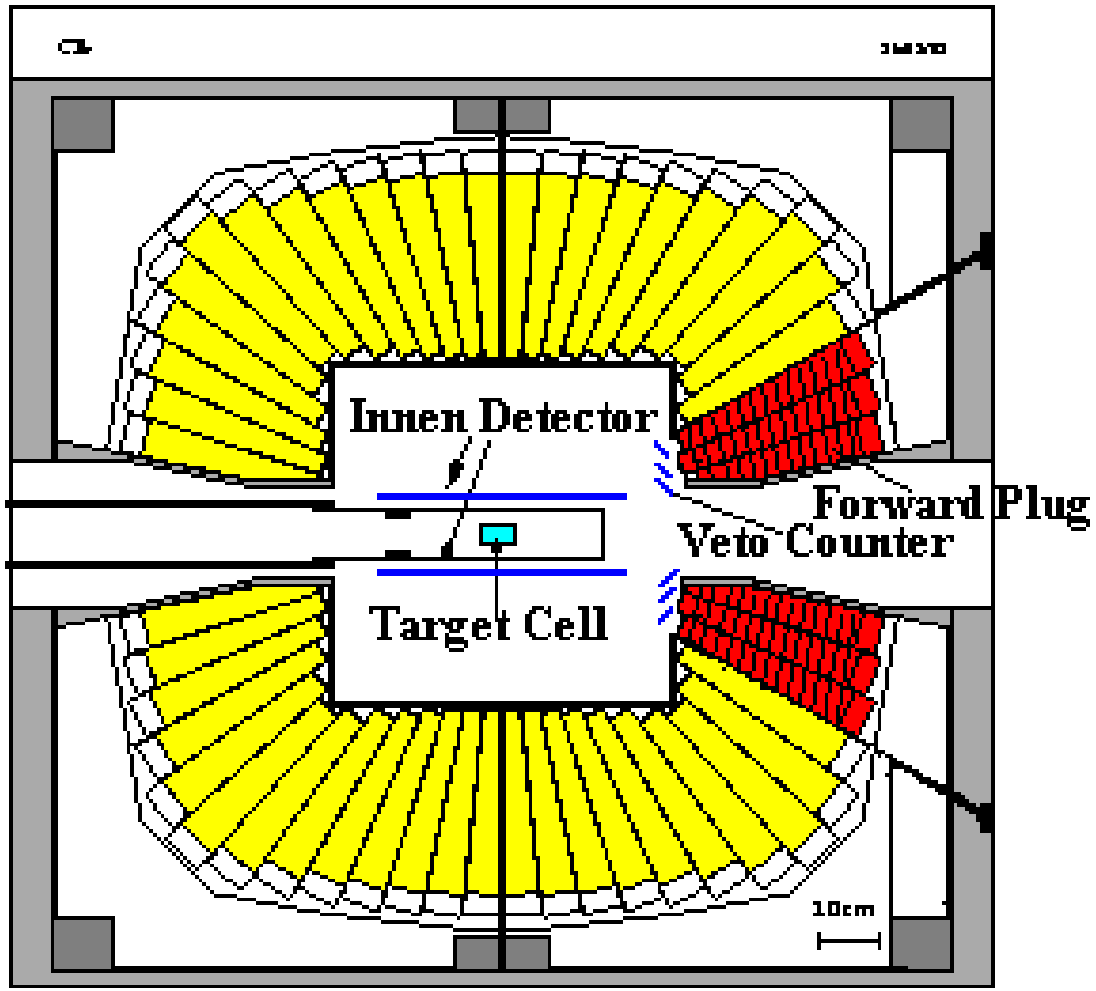

Verification of Energy Resolution

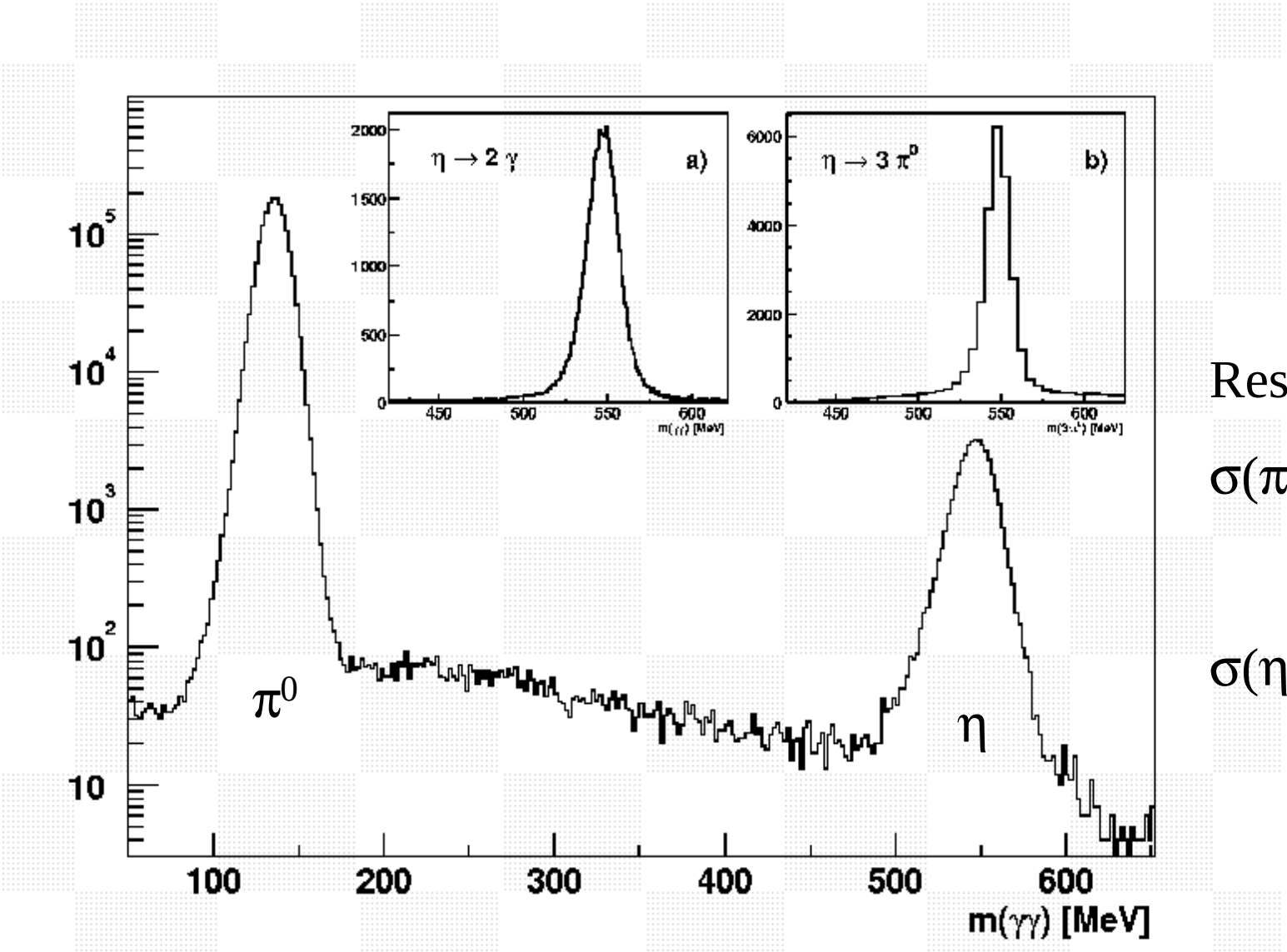

Resolution:

$\sigma(\pi^0) = 8{,}5$ MeV

(6,3 %)

$\sigma(\eta) = 12$ MeV

(2,2 %)

Baryons manifest the non-Abelian nature of the strong interaction. Thus, study of baryon excited states and production processes can provide insight into the dynamics and degrees of freedom relevant for non-perturbative quantum chromodynamics (QCD). At present, much of our limited understanding of these excited states comes from symmetric quark models [1,2]. These models predict a number of states with masses above 1.8 GeV that have not been observed in the πN channel [3], the so-called *missing resonances*. Photoproduction of multi-meson final states avoids πN in the initial and the final state and gives the opportunity to probe the sequential decays of such high-lying resonances. Especially in the regime of excited Δ states the $\Delta\eta$ final state is particularly attractive due to its isospin selectivity. Accordingly, the study of the photoproduction of multi-meson final states and in particular the reaction

$$\gamma \mathrm{p} \rightarrow \mathrm{p}\pi^0\eta \tag{1}$$

has gained in importance over the past years, both from the experimental side with the measurement of unpolarized total and differential cross sections [4,5,6,7,8] and the beam asymmetry Σ [5,9], as well as from the theoretical side. In the low-energy region, there have been attempts to treat the $\Delta(1700)D_{33}$ as resonance that is dynamically generated from Δ-η interactions [10], as well as attempts to understand the rapidly rising cross section [11] by formation of intermediate resonances. In the Bonn Gatchina partial wave analysis (BnGa-PWA), described in [12,13], evidence was reported for the $\Delta(1920)$, an established (three-star) resonance in the $J^P = 3/2^+$-wave and a not-well-known (one-star) resonance $\Delta(1940)$ with spin and parity $J^P = 3/2^-$ [6,7]. The two resonances seem to form a further parity doublet, possibly indicating a restoration of chiral symmetry at high baryon excitation masses [14]. The mass of the $J^P = 3/2^-$-state indicates a mild conflict with quark models [1,2] and is consistent with models describing QCD in terms of a dual gravitational theory, AdS/QCD [15,16].

Линейно поляризованный фотонный пучок взаимодействует с неполяризованной мишенью. Определение азимутального угла реакции f*.

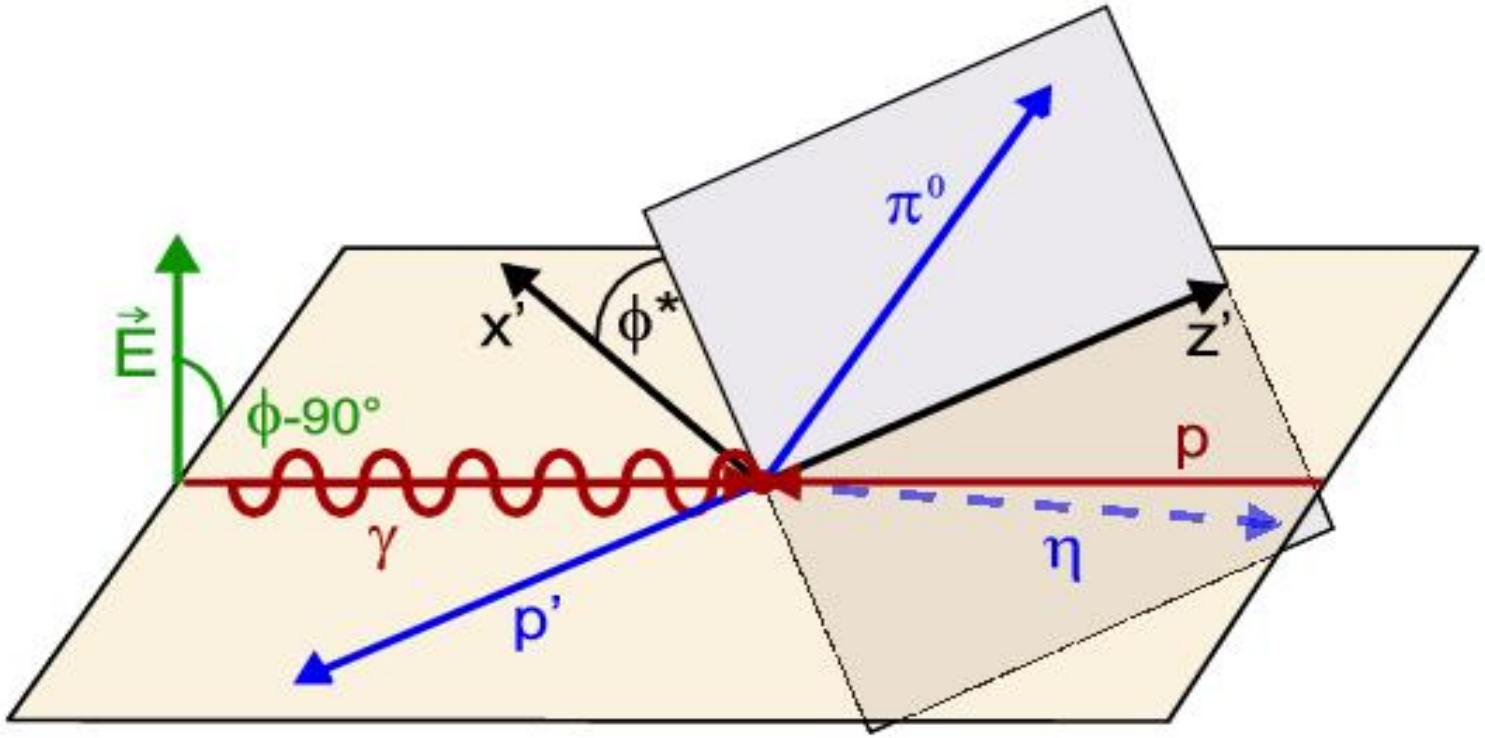

Fig. 1. Angle definitions in the center-of-momentum frame. ϕ^* is the angle between the reaction plane defined by the incoming photon and recoiling particle p' and the decay plane of two final state particles.

Сечение определяется формулой: $ds/dW = (ds/dW)_0 \{1+d_l[I^S \sin(2f) + I^C \cos(2f)]\}$

$(ds/dW)_0$ **- дифф. сечение в случае неполяризованного фотонного пучка.**

d_l **- степень линейной поляризации фотонного пучка;**

Выбраны интервалы энергий в системе центра масс:
1706 +/- 64 МэВ, 1834 +/- 64 МэВ, 1946+/- 48 МэВ.

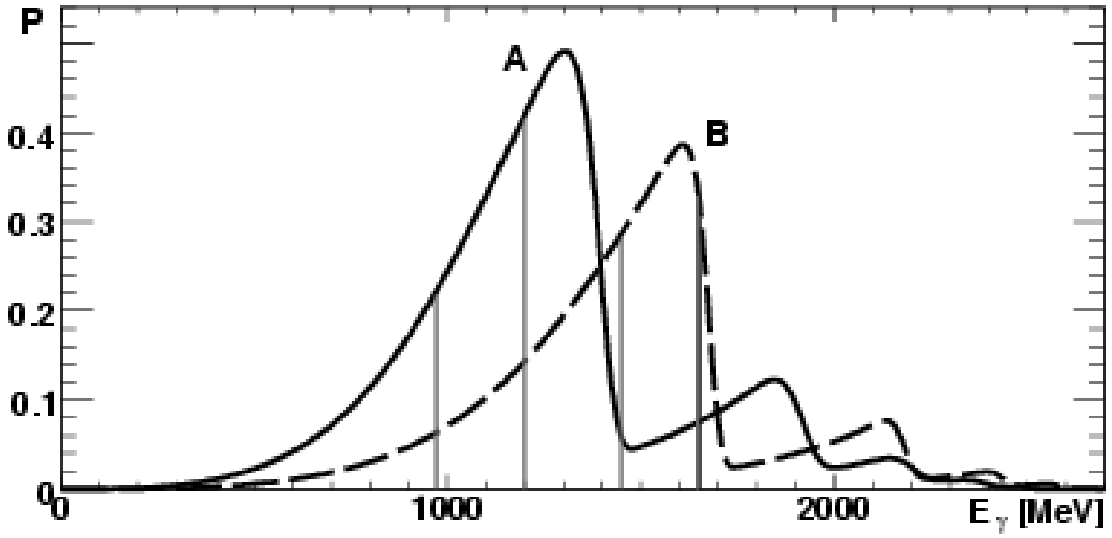

Fig. 2. Degree of linear polarization for the two settings. The largest polarizations were 49.2% at $E_\gamma = 1300\,\mathrm{MeV}$ (A) and 38.7% at 1600 MeV (B), respectively (see [27] for details). Vertical lines indicate the chosen energy ranges.

Two-meson photoproduction is not - like two-body reactions - restricted to a single plane as seen in Fig. 1; two planes, a reaction and a decay plane enclosing an angle ϕ^*, occur. In contrast to single-meson production, here polarization asymmetries can also occur if e.g. only the target is longitudinally polarized or if only the beam is circularly polarized. The first measurements of the latter asymmetries in double-pion photoproduction [17,18] have demonstrated their significant model sensitivity and revealed serious deficiencies of most available models. For linearly polarized photons impinging on an unpolarized target two polarization observables I^s and I^c occur, for which so far no data has been published in any channel. The latter corresponds to the polarization observable Σ if the dependence on the angle ϕ^* is integrated out. The cross section is written as

$$\frac{\mathrm{d}\sigma}{\mathrm{d}\Omega} = \left(\frac{\mathrm{d}\sigma}{\mathrm{d}\Omega}\right)_0 \{1 + \delta_l[I^s \sin(2\phi) + I^c \cos(2\phi)]\}, \qquad (2)$$

[19] where $\left(\frac{\mathrm{d}\sigma}{\mathrm{d}\Omega}\right)_0$ is the unpolarized cross section, δ_l is the degree of linear photon polarization, and ϕ the azimuthal angle of the reaction plane with respect to the normal on the polarization plane. Since polarization observables are very sensitive to interference effects in the amplitudes, they are expected to significantly constrain reaction models, and hence make the extraction of resonance parameters much more precise than unpolarized data alone would allow.

The data were obtained using the tagged photon beam of the ELectron Stretcher Accelerator (ELSA) [20] and the CBELSA/TAPS detector. The experimental setup consists of an arrangement of two electromagnetic calorimeters, the Crystal Barrel detector [21] comprising 1290 CsI(Tl) crystals and the TAPS detector [22,23] in a forward wall setup consisting of 528 BaF_2 modules in combination with plastic scintillators for charge information. Together these calorimeters cover the polar angular range from 5° to 168° and the full azimuthal range. For further charged particle identification a three layer scintillating fiber detector [24] surrounds the 5 cm long liquid hydrogen target [25]. The linearly polarized photons are produced via coherent bremsstrahlung of the initial 3.2 GeV electron beam off a diamond radiator. Electrons undergoing the bremsstrahlung process are then momentum analyzed using a tagging spectrometer consisting of a dipole magnet and a scintillator based detection system. For further details on the experimental setup, see [26].
For this analysis, two datasets were considered. Fig. 2 shows the degree of polarization as a function of the incident photon energy for two diamond radiator orientations. The systematic error of the polarization was determined to be $\Delta P \leq 0.02$ [27]. The two datasets were subdivided into three energy ranges, $W = 1706 \pm 64$ MeV, 1834 ± 64 MeV, and 1946 ± 48 MeV respectively, as indicated by the vertical lines in Fig. 2. To guarantee a sufficiently high degree of polarization, the low energy range consists solely of data taken with the polarization setting A, the high energy range of data taken with setting B. For the intermediate energy range, both datasets were combined. To select the reaction (1), events with five distinct hits in the calorimeters were considered in further analysis. Events were retained if at least one combination of four out of the five clusters was consistent with a π^0 and an η in the final state as determined by a 4σ cut on the corresponding two-particle invariant mass distributions. To avoid possible systematic effects due to scintillator inefficiencies,

charge information was not used to identify the proton. Instead, the direction of the fifth particle had to agree with the missing momentum of the supposed two-meson system; the angular difference had to be smaller than 10° in ϕ and, depending on the angular resolution in the polar angle of the calorimeters, 5° in θ for TAPS and 15° for the Crystal Barrel, respectively. Additionally the missing mass needed to be consistent with the proton mass within 4σ. After applying the preselection, the data was subjected to a kinematic fit [28] imposing energy and momentum conservation, assuming that the interaction took place in the target center. Only events that exceeded, according to the respective distributions, a probability (CL) of 8% for the $\gamma p \to p\pi^0\gamma\gamma$ two-constraint hypothesis and of 6% for the $\gamma p \to p\pi^0\eta$ three-constraint hypothesis, respectively, were retained. The proton direction resulting from the fit had to agree with the direction of the proton determined as stated above within 20°. In addition, events compatible with CL $> 1\%$ for the $\gamma p \to p\pi^0\pi^0$ hypothesis were rejected. The final event sample contains a total of 65431 events from reaction (1) with a maximum background contamination of 1% (Fig. 3). To extract the polarization observables defined in Eq. (2), the ϕ distribution of the final state particles was fit with the expression

$$f(\phi) = A + P\,[B\,\sin(2\phi) + C\,\cos(2\phi)], \tag{3}$$

with P being the polarization determined for each event individually

When investigating asymmetries, the detection efficiency is usually considered not to have an influence on the result. In the quotients B/A or C/A this drops out as long as the bins in the 5-dimensional phase space can be considered reasonably small compared to the variation of efficiency. If on the other hand the 5-dimensional phase space is not completely covered, which is true for most of the experiments, the given distributions represent only the polarization observable within the covered phase space. The acceptance for the CBELSA/TAPS experiment determined from MC simulations vanishes for forward protons leaving TAPS through the forward hole, and for protons going backward in the center-of-mass system, having very low laboratory momenta. To study these effects on the shown distributions, different MC datasets have been produced and analyzed. First of all a phase space MC dataset has been produced and was analyzed using the same analysis chain as for the data. A 2-dimensional acceptance and efficiency correction as function of the variables ϕ and ϕ^* has been determined. In addition, since effects due to the contributing physics amplitudes have to be considered, the result of the PWA discussed below has been used to study the acceptance and efficiency. The systematic error shown in Figs. 5 and 6 reflects the maximal effect determined by these methods. Given the statistical uncertainties of the data points the effects due to the acceptance and efficiency correction are small.

The sensitivity of the data to partial wave contributions is tested within the BnGa multi-channel partial wave analysis. The BnGa-PWA fits include a large number of reactions; a survey of the presently used datasets can be found elsewhere. Included in this fit were data on the reaction $\gamma p \to p\pi^0\eta$ but without information on I^s and I^c. The fit [6,7] had claimed evidence for contributions from negative- and positive-parity Δ resonances with spin $J = 3/2$, the $\Delta(1700)$ and the poorly established $\Delta(1940)$ resonances with $J^P = 3/2^-$, and the established $\Delta(1600)$ and $\Delta(1920)$ resonances with $J^P = 3/2^+$. The result of a new fit including I^s and I^c is shown in Figs. 5 and 6 as solid curves.

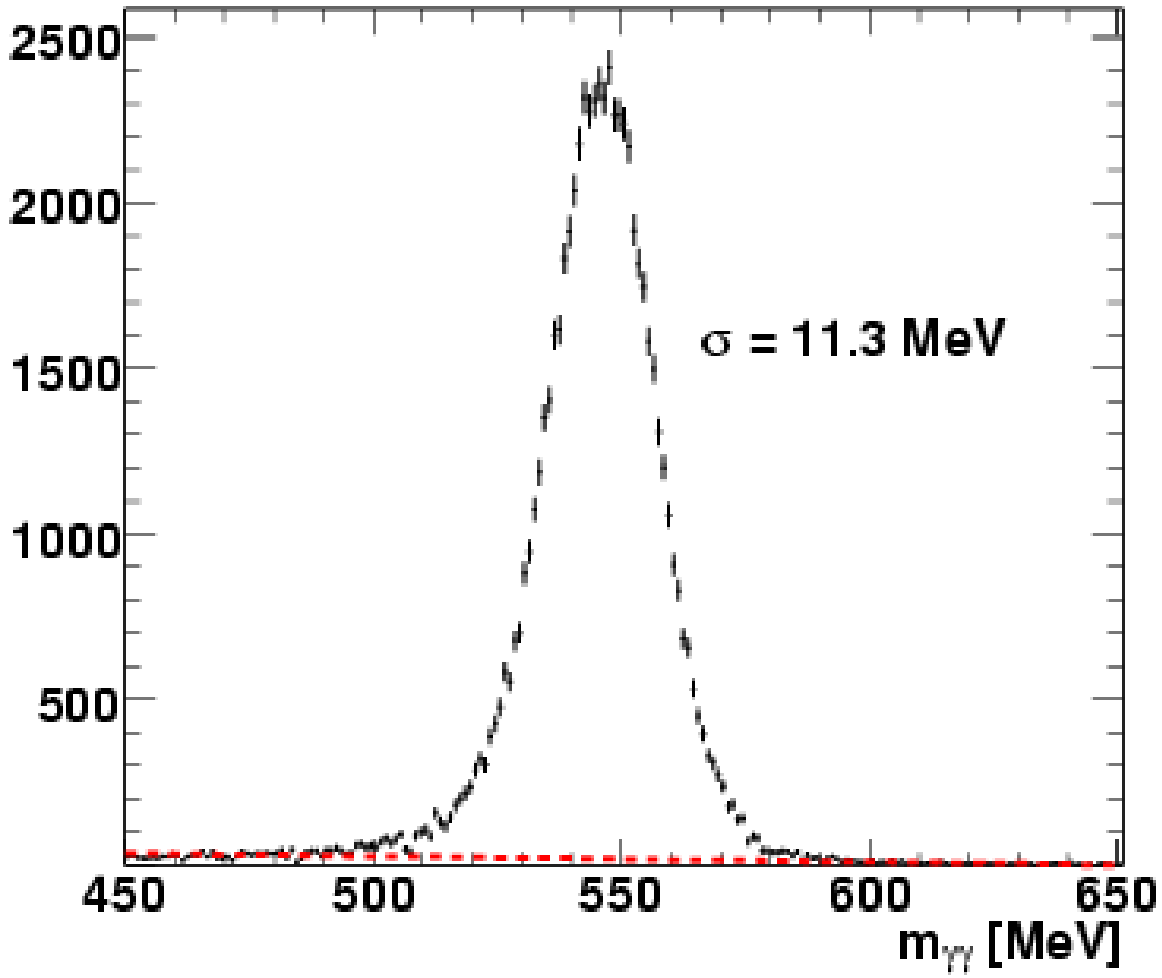

Fig. 3. $\gamma\gamma$ invariant mass distribution after cuts on the confidence levels of the $\gamma p \to p\pi^0\gamma\gamma$ (CL $>$ 8%) and $\gamma p \to p\pi^0\pi^0$ (CL $<$ 1%) fits respectively. This yields a total number of 68514 events including the linear background (red line). An additional cut on the $\gamma p \to p\pi^0\eta$ fit (CL $>$ 6%) rejects 3083 events, retaining 624 background events ($\approx$ 1%).

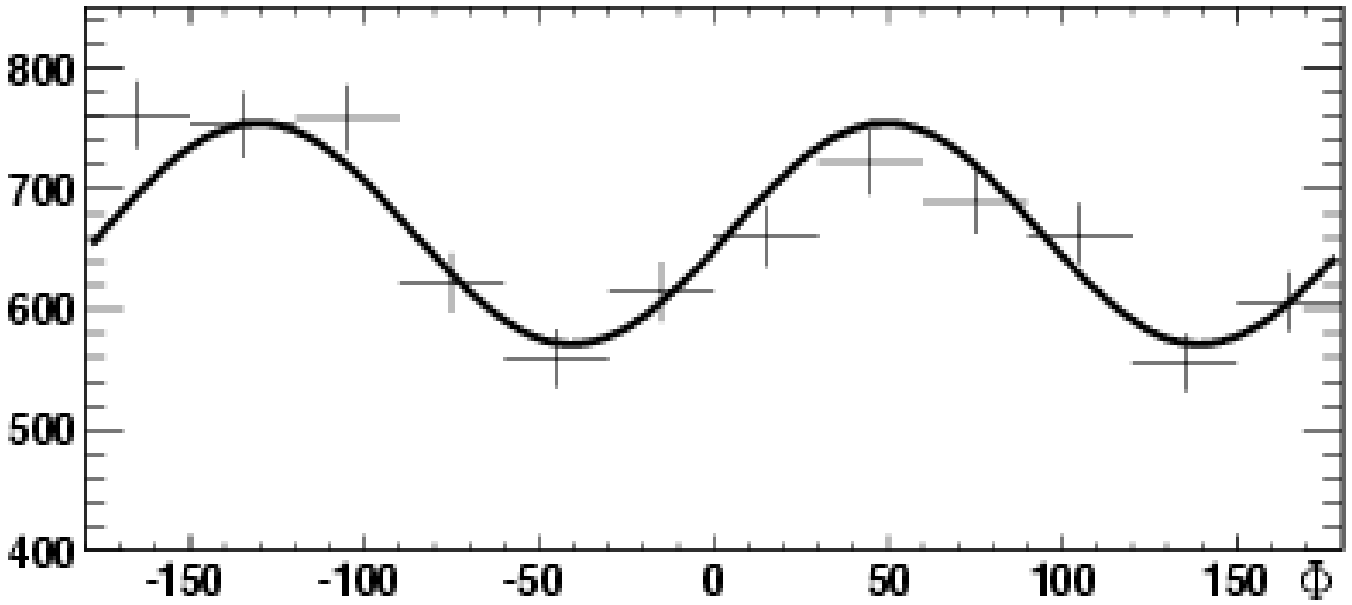

Fig. 4. Example of a measured ϕ-distribution. Shown is the ϕ-distribution of the final state proton in the region $60° \leq \phi^* \leq 120°$ for events in the energy range $W = 1834 \pm 64\,\mathrm{MeV}$ (y-axis with suppressed-zero scale).

Чувствительность поляризационных наблюдаемых к включению резонансов в ПВА. Штриховая кривая – ПВА Bonn-Gatchina не включает $3/2^-$ - парциальную волну, которая содержит Δ(1700) и Δ(1940) резонансы.

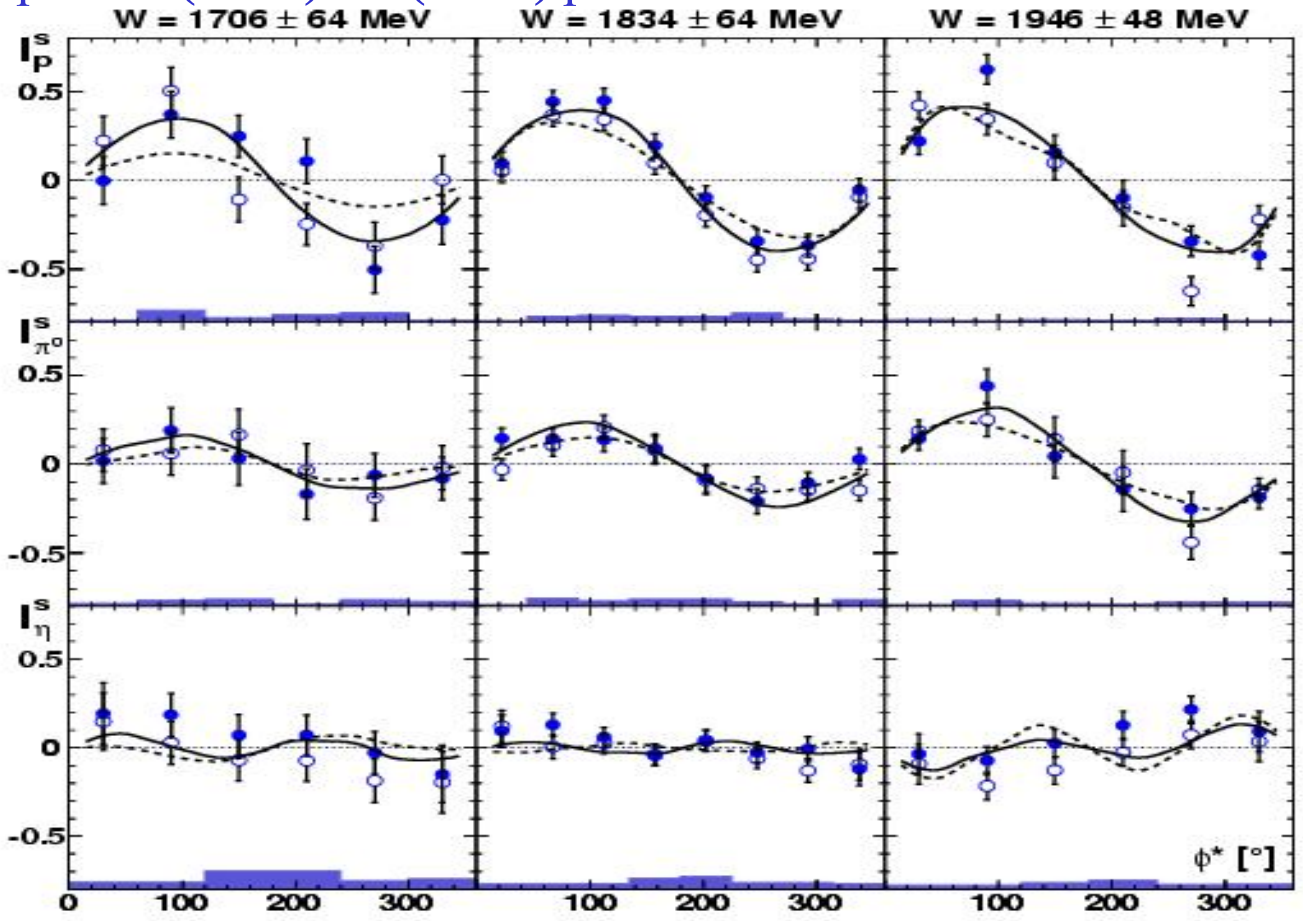

Fig. 5. Measured beam asymmetries I^s in the reaction $\vec{\gamma}p \to p\pi^0\eta$. Left to right: CMS energy ranges 1706 ± 64 MeV, 1834 ± 64 MeV, 1946 ± 48 MeV. Top to bottom: Beam asymmetries obtained treating the proton (top row), π^0 (center row) and η (bottom row) as recoiling particle. Filled symbols: $I^s(\phi^*)$, open symbols: $-I^s(2\pi-\phi^*)$. Solid curve: Full BnGa-PWA fit, dashed curve: BnGa-PWA fit excluding $3/2^-$-wave. Histograms below: Estimate of systematic errors due to acceptance and efficiency.

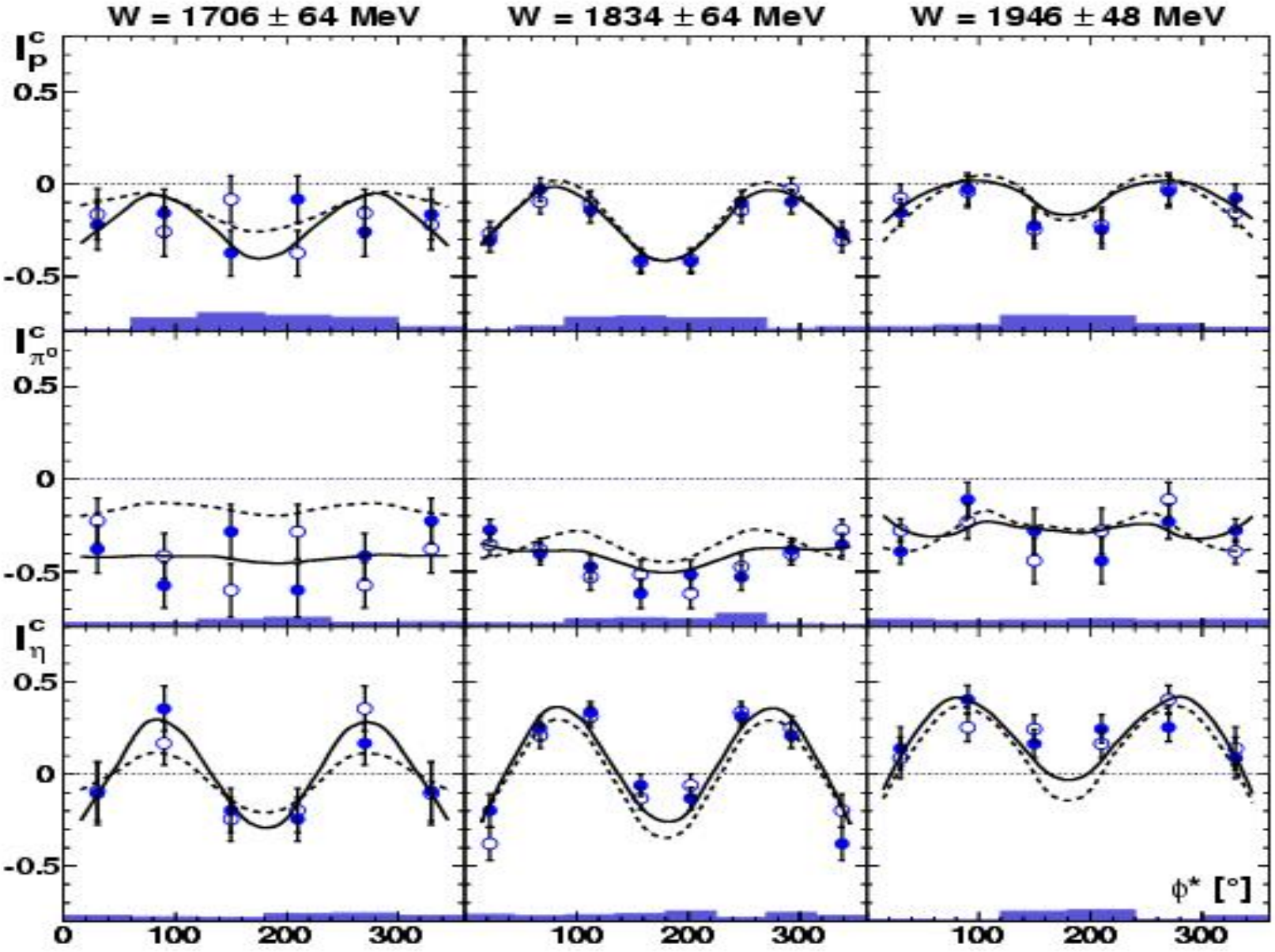

Fig. 6. Measured beam asymmetries I^c in the reaction $\vec{\gamma}p \to p\pi^0\eta$. Notation as Fig. 5, except filled symbols: $I^c(\phi^*)$, open symbols: $I^c(2\pi - \phi^*)$.

In addition to these fits within the BnGa-PWA, which demonstrate the sensitivity of I^s and I^c to the contributing partial waves, a preliminary comparison of the data with predictions using the chiral unitarity framework of [10] shows a significant relation between these new polarization observables and the production dynamics (1) [29]. Furthermore, discrepancies between these predictions and the data at higher energies point towards the need for additional contributions to be included in the model. These observations underline the importance of polarization observables in general and demonstrates the significance of I^s and I^c as new polarization observables in particular.

Статья 2010 год

Photoproduction of meson pairs: First measurement of the polarization observable I^S.

E. Gutz, V. Sokhoyan, H. van Pee, A.V. Anisovich, J.C.S. Bacelar, B. Bantes, O. Bartholomy, D. Bayadilov, R. Beck, Yu. Beloglazov, R. Castelijns, V. Crede, H. Dutz, D. Elsner, R. Ewald, F. Frommberger, M. Fuchs, Ch. Funke, R. Gregor, A. Gridnev, W. Hillert, Ph. Hoffmeister, I. Horn, I. Jaegle, J. Junkersfeld, H. Kalinowsky, S. Kammer, V. Kleber, Frank Klein, Friedrich Klein, E. Klempt, M. Kotulla, B. Krusche, M. Lang, H. Loehner, I. Lopatin, S. Lugert, D. Menze, T. Mertens, J.G. Messchendorp, V. Metag, M. Nanova, V. Nikonov, D. Novinski, R. Novotny, M. Ostrick, L. Pant, M. Pfeiffer, D. Piontek, W. Roberts, A. Roy, A. Sarantsev, S. Schadmand, Ch. Schmidt, H. Schmieden, B. Schoch, S. Shende, A. Suele, V. Sumachev, T. Szczepanek, A. Thiel, U. Thoma, D. Trnka, R. Varma, D. Walther, Ch. Weinheimer, et al. (1 additional author not shown)

Phys.Lett.B 687:11-15,2010